

How to Brake? Ethical Emergency Braking with Deep Reinforcement Learning

Jianbo Wang, Galina Sidorenko and Johan Thunberg *Member, IEEE*

Abstract—Connected and automated vehicles (CAVs) have the potential to enhance driving safety, for example by enabling safe vehicle following and more efficient traffic scheduling. For such future deployments, safety requirements should be addressed, where the primary such are avoidance of vehicle collisions and substantial mitigating of harm when collisions are unavoidable. However, conservative worst-case-based control strategies come at the price of reduced flexibility and may compromise overall performance. In light of this, we investigate how Deep Reinforcement Learning (DRL) can be leveraged to improve safety in multi-vehicle-following scenarios involving emergency braking. Specifically, we investigate how DRL with vehicle-to-vehicle communication can be used to ethically select an emergency breaking profile in scenarios where overall, or collective, three-vehicle harm reduction or collision avoidance shall be obtained instead of single-vehicle such. As an algorithm, we provide a hybrid approach that combines DRL with a previously published method based on analytical expressions for selecting optimal constant deceleration. By combining DRL with the previous method, the proposed hybrid approach increases the reliability compared to standalone DRL, while achieving superior performance in terms of overall harm reduction and collision avoidance.

Index Terms—Multi-vehicle safety, reinforcement learning, vehicle-to-vehicle communication, collision avoidance, automated driving.

I. INTRODUCTION

AUTONOMOUS vehicles (AVs) and connected such (CAVs) have been regarded a cornerstone of next-generation transportation systems, promising to reduce traffic accidents and fatalities through reliable automation strategies [1] [2]. Ensuring safety in multi-vehicle scenarios remains a critical challenge. Among various accident types, rear-end collisions, frequently caused by sudden deceleration of the leading vehicle, represent the most common and one of the most severe accident types [3].

Numerous control strategies have been proposed for multi-vehicle coordination in these settings [4] [5] [6]. Notably, [4] introduced a longitudinal safety framework based on extending the Responsibility-Sensitive Safety (RSS) model by explicitly calculating the minimum safe distance and the maximum safe communication latency/delay for specific scenarios. In [7], the benefit of vehicle-to-everything (V2X) communication in these settings is underscored; an algorithm for cooperative multi-vehicle safety is derived with a solution for minimum inter-vehicle distances (IVDs).

The authors are with the Department of Electrical and Information Technology (EIT), Lund University, SE-22100 Lund, Sweden (e-mail: ji0628wang@student.lu.se; galina.sidorenko@eit.lth.se; johan.thunberg@eit.lth.se).

This work was partially supported by the Wallenberg AI, Autonomous Systems and Software Program (WASP) funded by the Knut and Alice Wallenberg Foundation.

The approaches and schemes mentioned above rely on conservative strategies for worst-case scenarios, which undermines their safety performance. While safety in theory is guaranteed, the required inter-vehicle distance is inflated, and due to insufficient modeling and inflexible decision making avoidance of avoidable collisions may not be ensured in practice.

To overcome the limitations of the mentioned approaches in multi-vehicle scenarios, Deep Reinforcement Learning (DRL) emerges as a promising tool. By combining the decision-making framework of reinforcement learning with the function approximation capability of deep neural networks, DRL can effectively operate in high-dimensional and continuous-control domains [8]. Unlike classical methods, DRL agents learn control policies through direct interaction with the environment, optimizing cumulative rewards that explicitly encode safety objectives (e.g., penalizing collision risks and encouraging minimal collision harm) [9] [10]. This data-driven approach offers notable advantages, including the ability to handle non-convex and non-smooth Jacobian scenarios [11].

However, while prior studies [12]–[14] have demonstrated the effectiveness of DRL in various autonomous driving tasks (e.g., trajectory following, lane changing), its potential for improving *multi-vehicle rear-end collision mitigation* remains largely underexplored.

This paper focuses on emergency braking for three-vehicle longitudinal driving scenarios, a common and representative scenario for safe following in real-world traffic [15] [16], and one that is closely associated with the occurrence of rear-end collisions [17]. At the price of more coordination, three-vehicle interaction instead of pairwise interaction enables exploration of more degrees of freedom for improving safety. To address such scenarios, V2X communication is incorporated, with realistic communication delays and tight IVD to ensure the fidelity of the proposed method [18]. We consider a critical emergency braking situation where the leading vehicle encounters an unforeseen obstacle, triggering maximum deceleration (a_{\max}). This abrupt maneuver implies significant safety threats for the following vehicles due to severely reduced time-to-collision (TTC) and control latency caused by V2X communication delay/latency (τ). Beyond the safety challenges, this setting also embodies an ethical problem, underscoring the need for control strategies that minimize overall harm rather than prioritizing a single vehicle [19].

Based on this three-vehicle scenario, we propose a DRL-based approach that explicitly optimizes the ethical outcome expressed as overall harm. For rigorous performance evaluation, we use the method in [7], referred to as Ethical-V2X-Baseline Model (E-V2X-BM), as a benchmark. That method provides, via analytical expressions, overall harm as a function

of system parameters for an introduced braking strategy using constant deceleration for Vehicle 2. Evaluation results show that compared to this baseline method, our proposed approach reduces overall collision harm and, for certain IVDs, avoids collisions present for the E-V2X-BM.

As main algorithm, we develop a hybrid framework that integrates the learned DRL policy with the E-V2X-BM, leveraging V2X communication to enhance safety reliability in multi-vehicle driving scenarios. This hybrid design establishes a guaranteed safety bound while improving the robustness and reliability of DRL in practical deployment.

The contributions of this paper can be summarized as follows:

- **Application of DRL to Multi-Vehicle Longitudinal Safety:** We validate the applicability of the proposed DRL-based approach to collision avoidance in multi-vehicle longitudinal driving scenarios, training policies with multiple representative DRL algorithms. Compared to the existing ethical baseline, the proposed approach enhances overall safety by avoiding collisions in cases where the baseline fails and mitigating the severity when collisions are unavoidable.
- **Hybrid DRL Framework for Reliability:** We propose a hybrid framework that integrates the E-V2X-BM approach with DRL to achieve improved reliability. Within this framework, the proposed model serves as a guidance layer, steering decision-making toward balanced and reliable responses. Experimental results show that the hybrid design not only enhances E-V2X-BM performance but also achieves higher reliability compared to using DRL alone.

The remainder of this paper is structured as follows: Section II presents the problem statement, including the multi-vehicle longitudinal driving scenario and key safety considerations. Section III describes the DRL framework and the proposed hybrid approach. Section IV reports the experimental results including comprehensive evaluation metrics and analysis of the operational mechanisms behind safety improvements. Finally, Section V concludes the paper and discusses potential directions for future research.

II. PROBLEM STATEMENT

The main considered scenario is illustrated in Fig. 1. Three vehicles follow each other along a road. The leading vehicle is denoted Vehicle 1, the middle one Vehicle 2, and the last one Vehicle 3. We refer to $a_{l,i}^{\max}$ as the maximum deceleration magnitude, also referred to as braking capacity, for Vehicle i . It is assumed that the vehicles communicate with each other via V2X communication, enabling the sharing of relevant state, sensing, and emergency information. Without loss of generality, we assume that at time $t = 0$ Vehicle 1 has to emergency brake (to *e.g.*, avoid a potential collision with an unforeseen obstacle). Emergency braking in this context is modeled by Vehicle 1 decelerating with magnitude $a_{l,1}^{\max} > 0$. Due to latency and communication delays, Vehicle 2 starts braking at time $t = \tau_2 > 0$, while Vehicle 3 starts braking at time $t = \tau_3 > 0$. Vehicle 2 and Vehicle 3 can only

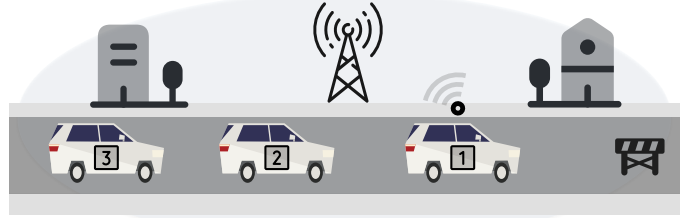


Fig. 1. Illustration of the Three-Vehicle Longitudinal Driving Scenario with V2X Communication.

brake in such a manner that their deceleration magnitudes do not exceed $a_{l,2}^{\max} > 0$ and $a_{l,3}^{\max} > 0$, respectively. The goal is to determine a feasible deceleration profile for Vehicle 2 that minimizes, and preferably avoids, collisions among the vehicles.

In this scenario, a simple braking strategy would be for Vehicle 2 and Vehicle 3 to apply their respective maximum braking capacities from time points τ_2 and τ_3 , respectively, until full stop. However, such a strategy would not necessarily be the least harmful one [7]. It might result in a collision that could potentially have been avoided with a more sophisticated braking strategy.

This paper considers the situation where Vehicle 3 applies maximum deceleration while Vehicle 2 applies a braking strategy learned via DRL. To be able to perform such a strategy, Vehicle 2 needs a small amount of information about Vehicle 1 and Vehicle 3 obtained via V2X communication. This information includes the maximum braking capacities and the initial states. In general, the braking strategy of Vehicle 2 should be chosen to ensure that all three vehicles stop safely without collisions. However, in extreme situations, such as tight IVDs, high velocities and/or high latencies, the objective shifts to selecting a strategy that reduces the collision severity or harm as much as possible.

In Section II-A we provide the system model, including vehicle dynamics, collision modeling, and the definition of harm resulting from a collision. Then, in Section II-B, we formalize the problem outlined above by formulating it as a discrete-time optimization problem for Vehicle 2, whose solution may be mapped to continuous time via interpolation.

A. System Model for emergency braking

Let $x_i(t)$ and $v_i(t)$ denote the position and velocity, respectively, of Vehicle i at time $t \in \mathbb{R}$, where $i \in \{1, 2, 3\}$. Since longitudinal motion is considered, the time evolution of the vehicles is modeled during collision-free intervals by:

$$\begin{bmatrix} \dot{x}_i(t) \\ \dot{v}_i(t) \end{bmatrix} = \begin{bmatrix} v_i(t) \\ u_i(t) \end{bmatrix} - a_{l,i}^{\max} \leq u_i(t) \leq a_{u,i}^{\max}, \quad i \in \{1, 2, 3\}, \quad (1)$$

where the control signal $u_i(t)$ (longitudinal acceleration/deceleration) is bounded from below and above.

At time $t = 0$, the leading vehicle (Vehicle 1) starts braking with maximum braking capacity until standstill:

$$u_1(t) = \begin{cases} -a_{l,1}^{\max}, & 0 \leq t \leq v_1(0)/a_{l,1}^{\max}, \\ 0, & t > v_1(0)/a_{l,1}^{\max}. \end{cases} \quad (2)$$

V2X communication introduces non-negligible latencies. We assume that Vehicle 3 has received and processed the message with the emergency braking information before the time-point τ_3 and starts braking at time $t = \tau_3$ with maximum braking capacity until standstill. Hence

$$u_3(t) = \begin{cases} 0, & t < \tau_3, \\ -a_{l,3}^{\max}, & \tau_3 \leq t \leq \tau_3 + v_3(0)/a_{l,3}^{\max}, \\ 0, & t > \tau_3 + v_3(0)/a_{l,3}^{\max}. \end{cases} \quad (3)$$

The middle vehicle (Vehicle 2) is a controllable agent that follows the control decision/policy $\pi_\theta(t)$ from time τ_2 onward. The symbol θ captures parameters to be learned for the policy. The time τ_2 is chosen sufficiently large to ensure that the necessary information for generating such control policy has been communicated from Vehicle 1 and Vehicle 3. This information comprises $a_{l,1}^{\max}$, $a_{l,3}^{\max}$, τ_3 , $v_1(0)$, $v_3(0)$, and relative distances $d_1(0) = x_1(0) - x_2(0)$, $d_2(0) = x_2(0) - x_3(0)$ (if they are not measured by onboard sensors of the ego vehicle). We also assume that Vehicle 2 is not involved in any collisions prior to time τ_2 . Thus, the control action of Vehicle 2 at emergency braking is given as

$$u_2(t) = \begin{cases} 0, & t < \tau_2, \\ \pi_\theta(\cdot), & t \geq \tau_2. \end{cases} \quad (4)$$

where $\pi_\theta(\cdot)$ is the deterministic policy, mapping the environment state to a control action in order to avoid collisions or mitigate their severity.

For $t > \tau_2$, the control input of Vehicle 2 must satisfy

$$-a_{l,2}^{\max} \leq u_2(t) \leq a_{u,2}^{\max}, \quad (5)$$

Furthermore, for $t > \tau_2$, the velocity shall satisfy

$$0 \leq v_2(t) \leq v_2^{\max} > 0, \quad (6)$$

which means that reverse motion is not possible and that the velocity is subject to an upper bound.

The relative distance between consecutive vehicles,

$$d_i(t) = x_i(t) - x_{i+1}(t), \quad i \in \{1, 2\} \quad (7)$$

is independent of the choice of global coordinate system and is used to define safety. Collision between Vehicle i and Vehicle $i+1$ implies that $d_i(t)$ becomes non-positive ($d_i(t) \leq 0$) for $i \in \{1, 2\}$. We define collision indicator function as follows

$$\Gamma(d_i) = \begin{cases} 1, & \text{if } d_i \leq 0, \\ 0, & \text{otherwise,} \end{cases}, \quad i \in \{1, 2\}, \quad (8)$$

where at time t , $\Gamma(d_i(t)) = 1$ indicates that a collision has occurred between Vehicle i and Vehicle $i+1$ for $i \in \{1, 2\}$. For the special case where $d_i(t) = 0$ and $v_i(t) - v_{i+1}(t) = 0$, the vehicles are merely touching without any energy exchange. As the present study focuses on collision harm, such a touching

scenario with zero relative velocity is considered to have no harm contribution and is therefore not counted as a collision.

A variety of metrics have been proposed for quantifying collision severity, from momentum exchange to detailed structural models [5], [20]. Empirical studies have demonstrated that the relative velocity between the two vehicles at the moment of collision is strongly correlated with the severity of the driver's injury [21], [22]. We define the relative velocity at time t as

$$\tilde{v}_i(t) = v_{i+1}(t) - v_i(t), \quad i \in \{1, 2\}. \quad (9)$$

At the collision time t_c , we denote $\tilde{v}_i^-(t_c)$ and $\tilde{v}_i^+(t_c)$ as the relative velocities immediately before and after the collision, respectively.

In [4], [5], [7] the relative velocity before the collision and the masses of the vehicles are combined to calculate a so-called harm coefficient. Here we use an energy-equivalent expression by using the square of the relative velocity. The harm $H_i(d_i, \tilde{v}_i)$ for Vehicle i , involved in a collision with Vehicle $i+1$ is defined as

$$H_i(d_i, \tilde{v}_i) = \left(\frac{m_{i+1}}{m_i + m_{i+1}} \tilde{v}_i^2 \right) \cdot \Gamma(d_i). \quad (10)$$

Similarly, the harm to Vehicle $i+1$ involved in a collision with Vehicle i is obtained as

$$H_{i+1}(d_i, \tilde{v}_i) = \frac{m_i}{m_{i+1}} H_i(d_i, \tilde{v}_i), \quad (11)$$

where the mass ratio term accounts for the distribution of kinetic energy between the two vehicles. With this notation, $H_2(d_1, \tilde{v}_1)$ is the harm for Vehicle 2 in a collision with Vehicle 1, whereas $H_2(d_2, \tilde{v}_2)$ is the harm for Vehicle 2 resulting from a collision with Vehicle 3.

To improve physical fidelity, the instantaneous change in velocities upon impact is modeled using the principle of conservation of momentum for the two vehicles. For a rear-end collision between Vehicle i and Vehicle $i+1$, the immediate after-collision velocities v_i^+ and v_{i+1}^+ satisfy

$$m_i v_i^+ + m_{i+1} v_{i+1}^+ = m_i v_i^- + m_{i+1} v_{i+1}^-, \quad (12)$$

where v_i^- denotes the velocity of Vehicle i before the collision for $i \in \{1, 2\}$.

Energy dissipation during the collision is modeled by using a coefficient of restitution $e \in [0, 1]$:

$$e = \frac{v_i^+ - v_{i+1}^+}{v_i^- - v_{i+1}^-}. \quad (13)$$

Thus, e is defined as the ratio of the relative velocity immediately after the collision to that before the collision. Its magnitude reflects the amount of energy dissipated during impact and depends on material properties, structural stiffness, and impact geometry. Empirical studies indicate that typical rear-end collisions correspond to $e \leq 0.3$ [23].

From (12) and (13), the following velocity exchange law is derived.

$$\begin{aligned} v_i^+ &= v_i^- + \frac{m_{i+1}}{m_{i+1} + m_i} (1 + e) \tilde{v}_i^- \\ v_{i+1}^+ &= v_{i+1}^- - \frac{m_i}{m_{i+1} + m_i} (1 + e) \tilde{v}_i^-. \end{aligned} \quad (14)$$

The formulation (14) provides an update rule for subsequent motion planning and collision severity assessment. As such, the dynamics of the system (which is partly described by (1)) is hybrid, where velocities jump to new values when relative positions are zero and relative velocities are positive.

B. Optimization Problem

To implement the DRL-strategy, we first discretize the dynamics of Vehicle 2. We then formulate an optimization problem, which incorporates the described model along with input constraints (5) and state constraints (6).

We use a zero-order hold discretization of (1) (see (15) below), where the sampling period is Δt and the continuous time signal is held constant between consecutive sampling instants. The time discretization begins at time $t = \tau_2$, thus discrete time instant n corresponds to the continuous time instant $t_n = \tau_2 + n\Delta t$. Furthermore, to capture the hybrid nature of the system, where velocities jump to new values at vehicle collision according to (14), the additional function \tilde{f} is used. This function comprises the composition of the two functions \tilde{f}_1 and \tilde{f}_3 , which capture collisions of Vehicle 2 with Vehicle 1 and Vehicle 3, respectively.

$$\underbrace{\begin{bmatrix} x_2(n+1) \\ v_2(n+1) \end{bmatrix}}_{s_2(n+1)} = \underbrace{\begin{bmatrix} 1 & \Delta t \\ 0 & 1 \end{bmatrix} \begin{bmatrix} x_2(n) \\ \tilde{f}(n, s_2(n)) \end{bmatrix}}_{f(s_2(n), u_2(n))} + \underbrace{\begin{bmatrix} (\Delta t)^2 \\ \Delta t \end{bmatrix} u_2(n)}, \quad (15)$$

where $s_2(n) = [x_2(n), v_2(n)]^\top$ denotes the state of Vehicle 2 at discrete time index $n \geq 0$ and

$$\tilde{f}(n, s_2(n)) = \tilde{f}_1(n, [x_2(n), \tilde{f}_3(n, s_2(n))]^\top), \quad (16)$$

where

$$\begin{aligned} \tilde{f}_1(n, s_2(n)) &= v_2(n) - \frac{m_1(1+e)}{m_2+m_1} \tilde{v}_1(n) \Gamma(d_1(n)), \\ \tilde{f}_3(n, s_2(n)) &= v_2(n) + \frac{m_3(1+e)}{m_2+m_3} \tilde{v}_2(n) \Gamma(d_2(n)). \end{aligned} \quad (17)$$

Here, $d_1(n)$ and $d_2(n)$ are defined by (7), $\tilde{v}_1(n)$ and $\tilde{v}_2(n)$ are defined by (9) with discrete time step n corresponding to $t_n = \tau_2 + n\Delta t$. The velocities of Vehicle 1 and Vehicle 3 are updated in an equivalent fashion when collisions with Vehicle 2 occur. Besides these events, Vehicle 1 and Vehicle 3 brake with constant deceleration (from time τ_3 for Vehicle 3) until standstill. Thus, their positions and velocities are regarded as functions of n and s_2 . Hence the updating rules at collisions are given as functions of n and s_2 only. For brevity, we do not provide the explicit discrete-time expressions for the positions and velocities of Vehicle 1 and Vehicle 3 as functions of n and s_2 ; these follow directly from (1), (2) or (3), and (14) together with discretization.

The objective function in the finite-horizon optimization problem with N time-steps comprises a sum of N terms

$$J = \sum_{n=0}^{N-1} J_n. \quad (18)$$

Each term J_n itself consists of two components

$$J_n = J_{\text{jerk},n} + J_{\text{harm},n}, \quad (19)$$

where both $J_{\text{jerk},n}$ and $J_{\text{harm},n}$ are functions of the state s_2 and the control input u_2 . For brevity, the explicit dependence on s_2 and u_2 is omitted in the provided definitions.

The first term, $J_{\text{jerk},n}$, promotes control smoothness and is defined as

$$J_{\text{jerk},n} = \left(\frac{u_2(n) - u_2(n-1)}{\Delta t} \right)^2. \quad (20)$$

The second component, $J_{\text{harm},n}$, penalizes severity of a collision when it is unavoidable, and is defined as

$$\begin{aligned} J_{\text{harm},n} &= H_1(d_1(n), \tilde{v}_1(n)) + H_2(d_1(n), \tilde{v}_1(n)) \\ &\quad + H_2(d_2(n), \tilde{v}_2(n)) + H_3(d_2(n), \tilde{v}_2(n)), \end{aligned} \quad (21)$$

where H_i for $i \in \{1, 2, 3\}$ is defined by (10) and (11). $J_{\text{harm},n}$ remains zero during safe driving but jumps to a (large) positive value if a collision occurs.

Finally, the finite-horizon, discrete-time, constrained optimal control problem over N time steps is formulated below

$$\left\{ \begin{array}{l} \text{minimize}_{\tilde{u}} J(\tilde{u}, \tilde{s}) = \sum_{n=0}^{N-1} J_n(\tilde{u}, \tilde{s}) \\ \text{s.t. } s_2(n) = f(s_2(n-1), u_2(n-1)), \\ \quad \text{for } n \in \{1, 2, \dots, N-1\}, \\ g(\tilde{s}, \tilde{u}) \leq 0, \\ \tilde{u} = [u_2(0), u_2(1), \dots, u_2(N-1)], \\ \tilde{s} = [s_2(0), s_2(1), \dots, s_2(N-1)]. \end{array} \right. \quad (22)$$

Here, function g captures state and input constraints provided in (5) and (6).

The objective function in the optimization problem (22) exhibits a non-convex and non-smooth Jacobian (due to collisions), making the application of traditional gradient-based optimizers computationally challenging. Therefore, we propose an adaptive Markov decision process (MDP) scheme based on the optimization problem (22) where the solution is obtained by using DRL. After this, we introduce a hybrid approach that combines DRL with a conservative control algorithm E-V2X-BM [7], yielding a policy that is both safer and ethically aligned.

III. DEEP REINFORCEMENT LEARNING (DRL) AND HYBRID DRL

In this section, we first introduce the essential concepts of DRL needed. We then present the learning algorithms used and subsequently discuss the detailed design of the Reinforcement Learning (RL) framework, including state space and reward shaping. Next, the hybrid method is proposed that combines the DRL approach with E-V2X-BM [7]. The purpose of the hybrid approach is to provide a runtime safety shield on the learned policy, delivering a safer and more reliable control strategy. The section ends with a description of the network architecture.

A. Deep Reinforcement Learning

DRL employs neural networks as function approximators and learns optimal policies through a closed-loop process of trial-and-error interactions guided by reward feedback. These

characteristics make DRL well-suited for multi-vehicle safe following problems [24] [25]. In practice, DRL policies are often realized using compact neural architectures – typically two- to four-layer Multilayer perceptrons (MLPs) – which incur low computational overhead. The networks directly output control actions, providing a one-to-one mapping that is highly suitable for embedded hardware. Empirical studies [26] [27] report inference latencies that satisfy vehicular control requirements, while hardware-oriented analyses [28] further confirm the feasibility of deploying such DRL controllers on resource-constrained devices.

Nevertheless, DRL suffers from a well-documented drawback: the black-box nature of its policies can undermine reliability in practical scenarios [29]. To overcome this limitation while preserving the practical advantages of DRL, we propose a hybrid approach that merges DRL with E-V2X-BM [7] that provides safety bounds through analytical expressions. This integration yields a robust and trustworthy braking control policy suitable for safety-critical vehicle-following scenarios.

B. DRL Algorithms Used

We use two DRL algorithms, Proximal Policy Optimization (PPO) [30] and Soft Actor-Critic (SAC) [31], briefly explained below. In Section IV we later compare the two choices of DRL algorithms.

PPO [30] is an on-policy reinforcement learning algorithm designed to improve policy performance while avoiding destabilizing with excessively large updates. It uses the importance sampling ratio and augments the standard policy-gradient objective with a clipping mechanism. The importance sampling ratio $\rho_n(\theta)$ is defined as:

$$\rho_n(\theta) = \frac{\pi_\theta(a_2(n) | s(n))}{\pi_{\theta_{\text{old}}}(a_2(n) | s(n))} \quad (23)$$

where θ_{old} and θ denote the parameters of the old (previous) and current policies, respectively; $a_2(n)$ and $s(n)$ is the action and the state, respectively, at timestep n . $\pi_\theta(a_2(n) | s(n))$ is a probability of action $a_2(n)$ under the current policy while $\pi_{\theta_{\text{old}}}(a_2(n) | s(n))$ denotes probability under the old policy. Further below, to save space, we denote the state at time step n by s_n instead of $s(n)$.

Clipping of $\rho_n(\theta)$ between $1 - \varepsilon$ and $1 + \varepsilon$ limits the maximum change between the old policy and the updated policy. The clipped objective is given by

$$\mathcal{L}^{\text{CLIP}}(\theta) = \mathbb{E} \left[\min(\rho_n(\theta) \hat{A}_n, \text{clip}(\rho_n(\theta), 1 - \varepsilon, 1 + \varepsilon) \hat{A}_n) \right] \quad (24)$$

where ε is the hyper parameter that controls the permissible deviation per update, and \hat{A}_n is the estimated advantage defined as:

$$\hat{A}_n = \sum_{l=0}^{\infty} (\gamma \lambda)^l \delta_{n+l}, \quad \delta_n = r_n + \gamma V_\theta(s_{n+1}) - V_\theta(s_n) \quad (25)$$

where γ is the discount factor, r_n is the reward at time instance n , λ is GAE parameter that keeps the balance of bias and variance, $V_\theta(s_n)$ is the value function corresponding to the state s_n at time step n , and δ_n represents the temporal-difference error.

Finally, the complete PPO loss function is given by:

$$\mathcal{L}^{\text{PPO}}(\theta) = \mathcal{L}^{\text{CLIP}}(\theta) - c_1 \mathbb{E}[(V_\theta(s_n) - V_{\text{target}})^2] + c_2 \mathbb{E}[\mathcal{H}(\pi_\theta)] \quad (26)$$

where c_1 and c_2 are loss coefficients, $\mathcal{H}(\pi_\theta)$ denotes the policy entropy, and V_{target} is the target value. By maximizing the \mathcal{L}^{PPO} in each iteration, PPO achieves stable updates, encourages exploration through the entropy term, and exhibits good convergence performance.

SAC, proposed in [31] and further developed in [32], is an off-policy, entropy-regularized reinforcement learning algorithm that jointly maximizes the expected return and policy entropy. It employs dual Q-critic architecture and a stochastic policy and an adaptive temperature parameter to maximize the expected return while maintaining sufficient exploration. The optimal policy is given by

$$\pi^* = \arg \max_{\pi} \sum_t \mathbb{E}_{(s_n, a_n) \sim \pi} \left[r_n + \alpha \mathcal{H}(\pi(\cdot | s_n)) \right] \quad (27)$$

where $\mathcal{H}(\pi(\cdot | s_n)) = -\mathbb{E}_{a \sim \pi} [\log \pi(a | s_n)]$ denotes the policy entropy, and $\alpha > 0$ is a temperature coefficient that balances exploration and exploitation.

In the follow-up work [32], to automatically adjust the temperature parameter α is treated as a learnable parameter, updated via entropy-constrained optimization:

$$\alpha_n^* = \arg \min_{\alpha_n} \mathbb{E}_{a_n \sim \pi_n^*} \left[-\alpha_n \log \pi_n^*(a_n | s_n, \alpha_n) - \alpha_n \bar{\mathcal{H}} \right] \quad (28)$$

where $\bar{\mathcal{H}}$ is a predefined target entropy.

Entropy regularization, combined with the twin-critic design, provides SAC with stable exploration and robust convergence, making it particularly effective for high-dimensional, safety-control tasks considered in this work.

C. MDP formulation

The three-vehicle following scenario is abstracted as an MDP where essential components are described below.

State: the system state or observation $s(n)$ comprises the (deterministic) actions of other vehicles and positions and velocities of all vehicles.

Action: in the problem considered, the RL agent controls only Vehicle 2. At each time step, the policy outputs

$$a_2 \in [-a_{l,2}^{\max}, a_{u,2}^{\max}] \subset \mathbb{R}, \quad (29)$$

where the scalar action a_2 is the longitudinal acceleration/deceleration applied to the ego vehicle. The actions a_1 and a_3 are deterministic and given by (2) and (3), respectively.

Transition: $\mathcal{P}(s(n+1) | s(n), a_2(n))$ captures the dynamics (15).

Reward: Reward shaping is done by modifying $J(\tilde{u}, \tilde{s})$ in (22) and reversing its sign so that maximizing the return corresponds to minimizing the objective. Additional shaping terms are introduced to facilitate learning. All-in-all, the reward comprises four components that are added together. These terms are explained below.

Collision-severity penalty: this term, which corresponds to $J_{\text{harm},n}$ (21), penalizes collisions by generating a large cost proportional to the relative velocity:

$$r_{\text{collision}} = - \sum_{i=1}^2 k_{\text{energy},i} (\tilde{v}_i(n))^2 \Gamma(d_i(n)), \quad (30)$$

where $\tilde{v}_i(n)$ is defined by (9), and $k_{\text{energy},i}$ are weight coefficients for $i \in \{1, 2\}$ that balance the importance of this penalty relative to other reward components.

Collision-risk penalty: to explicitly capture collision risk and provide tense penalties during training, both from the leading and following vehicles, we adopt a TTC-based penalty in combination with a distance-based shaping term. Given the relative distance d_i and relative velocity \tilde{v}_i , the instantaneous collision risk is defined as:

$$r_{\text{risk}} = \sum_{i=1}^2 \left(-\sigma \left(-\frac{\text{TTC}_i}{\tau} \right) + \underbrace{-\sigma(k_d(d_{\text{target}} - d_i))}_{\text{Distance penalty}} \right), \quad (31)$$

where $\text{TTC}_i = \frac{d_i - d_{\text{safe}}}{\tilde{v}_i}$ is the estimated time to collision, \tilde{v}_i is defined by 9, $k_d > 0$ is a scaling coefficient, $d_{\text{safe}} \geq 0$ is the safety buffer, $d_{\text{target}} \geq 0$ is the target safe distance, and $\tau > 0$ acts as a time-scaling factor in the TTC term. Here, σ denotes the sigmoid function $\sigma(x) = \frac{1}{1+e^{-x}}$. It is introduced to bound the risk terms within a finite range, ensuring numerical stability during training and providing smooth gradients that facilitate policy optimization [33].

Control-smoothness penalty: this term, corresponding to $J_{\text{jerk},n}$, aims to avoid overly aggressive control input:

$$r_{\text{jerk}} = -J_{\text{jerk},n} \quad (32)$$

Terminal reward: to encourage safe completion of an episode, a sparse constant reward is granted whenever the episode terminates without any collisions:

$$r_{\text{terminal}} = \begin{cases} R_{\text{safe}}, & \text{if no collision} \\ 0, & \text{otherwise.} \end{cases} \quad (33)$$

Therefore, the total reward is defined as:

$$r_{\text{total}} = w_h r_{\text{collision}} + w_p r_{\text{risk}} + w_j r_{\text{jerk}} + r_{\text{terminal}} \quad (34)$$

where w_h , w_p , and w_j are nonnegative weighting coefficients that balance collision avoidance, risk sensitivity, and motion smoothness, respectively.

D. Hybrid DRL with E-V2X-BM

In [4], the method we refer to as E-V2X-BM was proposed for assessing and improving safety in emergency braking for the three-vehicle following scenario. This method is based on analytic expressions. The setting in [4] was similar to the one considered in this paper, but the deceleration of Vehicle 2 was assumed to be constant and did not vary during braking.

In E-V2X-BM, analytical expressions are used to implement an algorithm that allows to calculate the so-called expected harm H_{total} for all three vehicles, depending on the control input of Vehicle 2. This expected harm is equal to the overall harm or total harm we consider in this paper. We will

henceforth simply refer to it as harm. The provided analytical functions depend on the initial IVDs $d_i(0)$, velocities, $v_i(0)$, deceleration capabilities $a_{l,i}^{\text{max}}$, and the V2X delays τ_i for all i . Given the calculated H_{total} , the minimum of the harm can be found, $H_* = \min_{a_2} H_{\text{total}}(a_2)$, as well as the corresponding deceleration magnitude a_* :

$$a_* = \arg \min_{a_2} H_{\text{total}}(a_2). \quad (35)$$

In scenarios where collisions can be avoided, i.e., $H_* = 0$, the corresponding constant deceleration is possible to choose from an interval. That is, any constant deceleration a_* within this interval guarantees a collision-free stop. When no constant deceleration results in a collision-free scenario, a_* is uniquely determined as the deceleration that minimizes harm.

We use H_* as a harm baseline which is used as a benchmark against DRL-based strategies. Furthermore, H_* is used as a safety threshold in the proposed hybrid approach. Any DRL output with harm exceeding this threshold is automatically rejected. Compared to using reinforcement learning only, this provides a lightweight mechanism that is provably safe, transparent, and reliable; a hybrid control framework that integrates DRL with E-V2X-BM to achieve high performance with reliability.

The hybrid algorithm includes two essential components:

- 1) *Safety Bound.* When the prediction horizon contains no imminent collision, the DRL output a_{RL} is executed directly. If an emergency is expected, the harm H_* is computed with the E-V2X-BM approach.
- 2) *Actor Layer.* The actor π_{RL} is implemented as a two-layer ReLU network that outputs a control command u_2 at each timestep. If the prediction horizon contains no imminent collision, u_2 is executed directly.

The two components operate as follows: once an emergency is detected, the algorithm compares the predicted harm of the actor's output with that of E-V2X-BM, i.e., H_* , and selects the strategy with the lowest harm as the final strategy. Specifically, upon receiving an emergency braking alert, Vehicle 2 immediately executes Algorithm 1. First, the safety bound H_* is calculated, with the use of real-time V2X measurements (headway, velocities, and communication delays). Then, the harm H_{RL} for the DRL policy is computed. The result is then compared against the safety bound H_* to produce the safe decision β_{safe} , where $\beta_{\text{safe}}=1$ corresponds to selecting the DRL policy and $\beta_{\text{safe}}=0$ to selecting the E-V2X-BM baseline.

E. Network Architecture

In this paper, a lightweight multilayer perceptron is used to train the policy π_{θ} . Specifically, the policy network consists of two fully connected hidden layers, each with a width of 256 nodes, followed by a ReLU activation function. In PPO framework, the value network $V_{\phi}(s)$ that is trained to approximate value function has an additional hidden layer with 128 nodes to enhance its ability to approximate higher-order value functions. In SAC framework, both the policy network and the double Q network adopt a symmetrical structure: two fully connected hidden layers, each with 256 nodes, using ReLU activation function.

Algorithm 1 Hybrid method

Input: State $s(n)$.

Output: Control sequence $\{u_2(n)\}$

- 1: Compute Safety baseline (a_*, H_*) by Eq. 35
- 2: Set initial RL command $a_{RL} \leftarrow \pi_{RL}(s(n))$
- 3: Set expected harm $H_{RL} \leftarrow 0$
- 4: **for** $n = 1$ to N **do**
- 5: Predict next state under current RL action a_{RL} :
 $s' \leftarrow \mathcal{P}(s(n), a_{RL})$
- 6: Update RL command for the predicted state:
 $a_{RL} \leftarrow \pi_{RL}(s')$
- 7: **if** COLLISION **then**
- 8: Compute step harm
 $H_n \leftarrow H(s')$ by Eq. (21)
- 9: **end if**
- 10: Update expected harm:
 $H_{RL} = H_{RL} + H_n$
- 11: **end for**
- 12: **Decision:**
- 13: **if** $H_{RL} \leq H_*$ **then**
- 14: Select DRL strategy: $\beta_{safe} \leftarrow 1$
- 15: **else**
- 16: Select E-V2X-BM strategy: $\beta_{safe} \leftarrow 0$
- 17: **end if**
- 18: **return** Based on β_{safe} , select the strategy to generate the control sequence $\{u_2(n)\}$.

IV. EXPERIMENTAL RESULTS AND OBSERVATIONS

This section first establishes the feasibility of applying DRL to the three-vehicle safety scenarios considered. Then, the effectiveness and reliability of the proposed hybrid method is validated. Finally, multi-episode simulations demonstrate that DRL-based approaches reduce collision harm and improve safe car-following performance compared with E-V2X-BM.

A. Experimental Set-Up

A three-vehicle emergency braking simulation platform is used for training and evaluation. The two different DRL algorithms described in Section III-B, SAC and PPO, are used for policy learning with hyperparameters summarized in Table I. In the evaluation, the proposed DRL-based approaches and the hybrid safety method are compared against two baselines: the E-V2X-BM method and a non-ethical driving policy where Vehicle 2 applies maximum possible deceleration during braking to increase the distance from Vehicle 1 in front. Given the primary emphasis on safety, collision harm calculated by (10) is selected as the principal performance metric. For fair comparison, we follow the protocol presented in [4] for the E-V2X-BM method, where the harm associated with each pairwise collision is counted only once.

To facilitate reproducibility and further research, the complete environment configuration, including vehicle dynamics configurations, parameter weights and the detailed reward-function design, will be available on GitHub.

TABLE I
PPO AND SAC HYPERPARAMETERS

| Parameter | Algorithm | Value |
|-----------------------------------|-----------|------------|
| Policy | PPO/SAC | MlpPolicy |
| Learning rate | PPO/SAC | cosine |
| γ | PPO/SAC | 0.99 |
| Device | PPO/SAC | CPU |
| Activation function | PPO/SAC | ReLU |
| PPO | | |
| n_{steps} | PPO | 2048 |
| n_{epochs} | PPO | 4 |
| Batch size | PPO | 512 |
| Clip range, ε | PPO | 0.15 |
| GAE, λ | PPO | 0.95 |
| Value function coefficient, c_1 | PPO | 0.5 |
| Entropy coefficient, c_2 | PPO | 0.005 |
| Target KL divergence | PPO | 0.15 |
| Maximum gradient norm | PPO | 0.3 |
| SAC | | |
| Batch size | SAC | 256 |
| Buffer size | SAC | 10^6 |
| Learning starts | SAC | 10^4 |
| Target smoothing τ | SAC | 0.02 |
| Training frequency (steps) | SAC | Every step |
| Gradient steps per update | SAC | 1 |
| Entropy coefficient, α | SAC | auto |
| Target update interval (steps) | SAC | 1 |

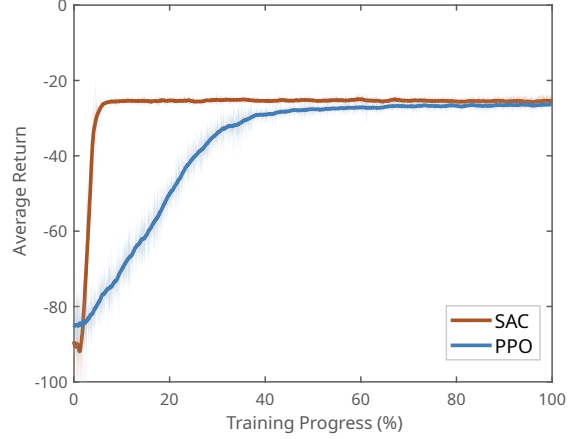


Fig. 2. Training performance of PPO and SAC algorithms under high-latency conditions. The horizontal axis corresponds to the training progress (%), and the vertical axis corresponds to the average return.

B. Learning Feasibility

Fig. 2 shows the reward curves for PPO and SAC for scenarios with large V2X communication delays, while Fig. 3 depicts the corresponding reward curves for small delays. The solid lines denote the mean average return, and the shaded areas show the standard deviation over multiple training tests with different random seeds.

In the high-delay case, both algorithms achieve steady convergence in the average return, with the final return values being nearly identical across different delay settings. This can be attributed to the fact that under high V2X latency, short available braking time limits the controllable window for policy. This results in more severe collisions and therefore limits

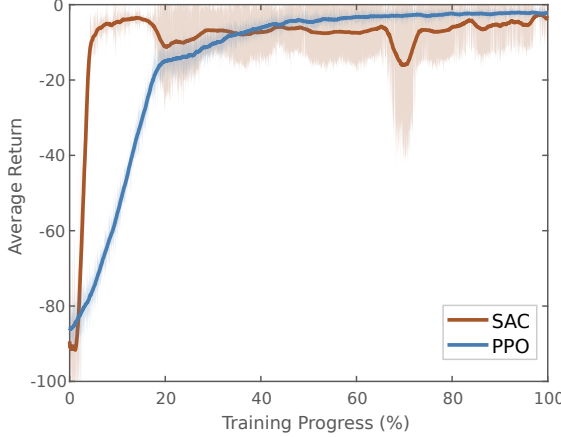


Fig. 3. Training performance of PPO and SAC algorithms under low latency conditions.

the room for performance improvements through learning.

When the time delay is small, SAC exhibits a faster convergence than PPO, whereas PPO exhibits more stable convergence than SAC. Both DRL algorithms achieve higher returns than in the high-latency case, indicating improved safety under low-delay conditions. This improved safety performance for small time delays is mainly due to an extended time window available for decisions.

The training curves show higher variance when the delay is low. This mostly stems from the sparse-reward design: as more controllable scenarios are introduced, positive rewards occur intermittently and in bursts, which amplifies fluctuations in returns and, consequently, in the policy updates [34] [35].

From an application perspective, these results imply that PPO may be a more suitable choice for deployment in high-latency scenarios where stability is critical, while SAC is to be preferred in low-latency environments where faster convergence is desired.

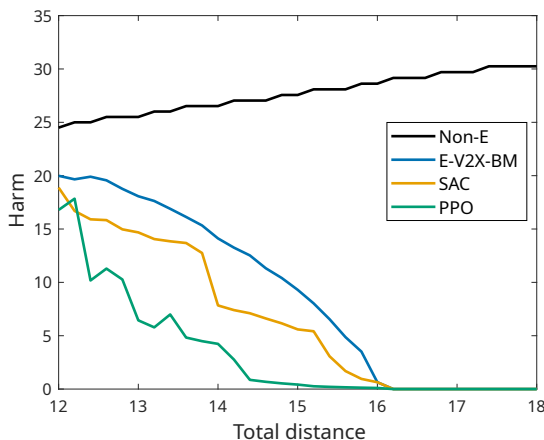


Fig. 4. Comparison of harm across four control strategies: Non-ethical, E-V2X-BM, and the DRL methods SAC and PPO. The horizontal axis shows the sum of initial IVDs, i.e. $d_1(0) + d_2(0)$, referred to as total distance, and the vertical axis shows harm.

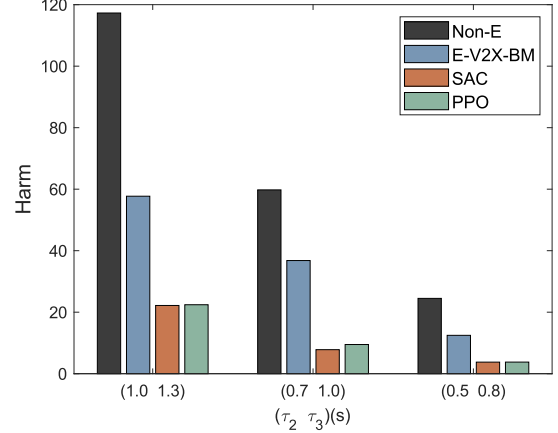


Fig. 5. Harm comparison for four control strategies under different V2X delays, (τ_2, τ_3) .

C. Standalone DRL

For the safety performance evaluation, we compared the severity of collisions (harm) to two different control strategies. The first is a non-ethical approach, where each vehicle applies maximum braking until standstill or collision at the times $0, \tau_2$ and τ_3 for Vehicle 1, Vehicle 2 and Vehicle 3, respectively. The second is the E-V2X-BM method. The two methods provide reference points for evaluating the two standalone (i.e., not the hybrid method) DRL strategies, i.e., SAC respective PPO.

In Fig. 4 a comparison is shown of the collision severity or harm as function of $d_1(0) + d_2(0)$, referred to as total distance, for the four control strategies when $v_1(0) = 20$ m/s, $v_2(0) = 18$ m/s, $v_3(0) = 20$ m/s, $\tau_2 = 0.5$ s, $\tau_3 = 0.8$ s, $a_{l,1}^{\max} = a_{u,1}^{\max} = a_{l,3}^{\max} = a_{u,3}^{\max} = 6$ m/s², $a_{l,2}^{\max} = a_{u,2}^{\max} = 7$ m/s², $m_1 = 4.5$ t, $m_2 = 5.5$ t, $m_3 = 5.9$ t. Here random IVDs are selected for each choice of total distance and average harm is presented. The non-ethical strategy has the highest harm, remaining large throughout IVDs sum test range. The perhaps non-intuitive result for the non-ethical strategy that larger IVDs correspond to larger average harm is due to the fact that $a_{l,2}^{\max} > a_{l,3}^{\max}$. Since Vehicle 2 brakes earlier and harder than the Vehicle 3, an initial IVD $d_2(0)$ allows (statistically speaking) the relative velocity between Vehicle 2 and Vehicle 3 to be larger at collision.

The E-V2X-BM strategy reduces harm compared to the non-ethical method, but still suffers from high collision severity for short initial IVDs, reflecting the limitations of selecting a constant deceleration for Vehicle 2. Both SAC and PPO strategies achieve lower average harm compared to the E-V2X-BM strategy across the entire IVDs range.

Fig. 5 presents harm values for the four strategies under three different communication delay configurations, where the initial IVDs are $d_1(0) = d_2(0) = 7$ m, and all other settings as in the previous scenario. Both SAC and PPO consistently achieve the lowest harm values across all tested delay setting, demonstrating strong robustness to increased communication latency.

To further examine the detailed operational behavior of the control strategies, simulation experiments are performed under

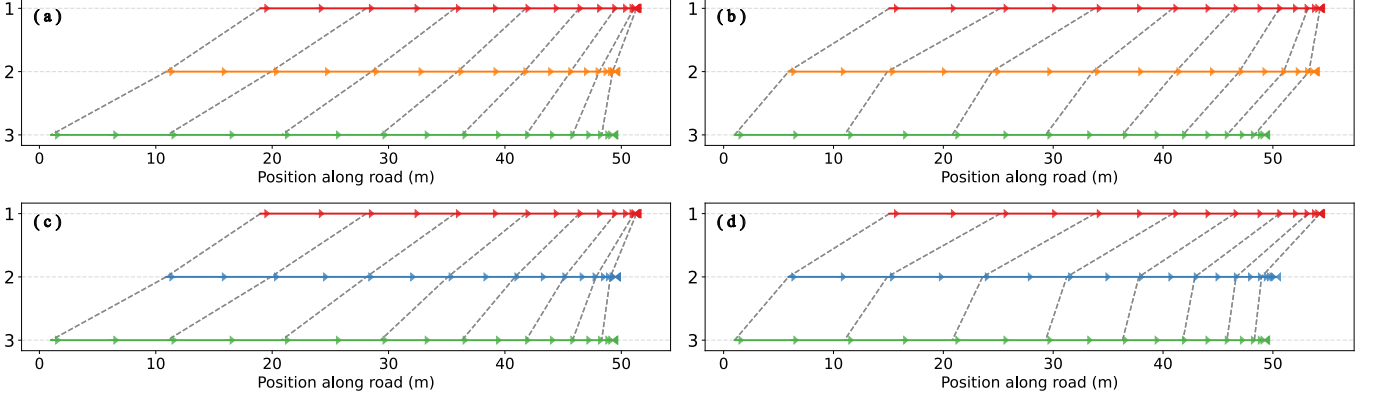


Fig. 6. Vehicle trajectories for two scenarios, Scenario 1 and Scenario 2. For each subplot, the x-axis shows the position along the road in meters, and the y-axis denotes the vehicle index. (a) and (b) correspond to PPO in Scenario 1 and 2, respectively, while (c) and (d) correspond to SAC in Scenario 1 and 2, respectively.

two sets of initial conditions. Figure 6 presents the resulting vehicle-following trajectories for PPO and SAC. For clarity, the positions of the three vehicles along the road are illustrated as parallel lines, with vehicle headings indicated by arrows at every tenth time step. Dashed lines connect the positions of the vehicles for the same time steps, showing their relative spacing.

For subplots (a) and (c), the initial IVDs are $d_1(0) = 10$ m and $d_2(0) = 8$ m, and the initial velocities are $v_1(0) = 20$ m/s, $v_2(0) = 18$ m/s, and $v_3(0) = 20$ m/s. For subplots (b) and (d), the corresponding initial values are $d_1(0) = 5$ m, $d_2(0) = 9$ m, $v_1(0) = 22$ m/s, $v_2(0) = 18$ m/s, and $v_3(0) = 20$ m/s.

In Fig. 6, it can be observed that vehicle positions are similar for SAC and PPO in Scenario 1. However, in Scenario 2, despite identical reward shaping and parameter settings, the two DRL algorithms result in noticeably different positioning. For Vehicle 2, PPO provides a policy that prioritizes maintaining a larger distance to Vehicle 3, while SAC provides a policy that prioritizes maintaining a larger distance to Vehicle 1.

Fig. 7 shows the control strategies obtained from PPO and SAC that produce the vehicle positions in Fig. 6. Subplots (a) and (c) in Fig. 7 show similar patterns, which was also observed for the corresponding subplots (a) and (c) in Fig. 6. In contrast, subplots (b) and (d), corresponding to (b) and (d) in Fig. 6, show distinct behaviors for Scenario 2; for PPO the control strategy involves an initial acceleration prior to maximum braking, whereas SAC exhibits deceleration throughout most of the scenario. For scenario 2, despite being trained with the same reward shaping, the PPO policy produces a smoother acceleration/deceleration profile compared to SAC.

D. Hybrid Method

This section presents an evaluation of the proposed hybrid approach that combines DRL with E-V2X-BM. Figure 8 captures the concept of the hybrid approach. The green curve is the harm for E-V2X-BM as a function of total distance (i.e., $d_1(0) + d_2(0)$), while the orange curve is the harm

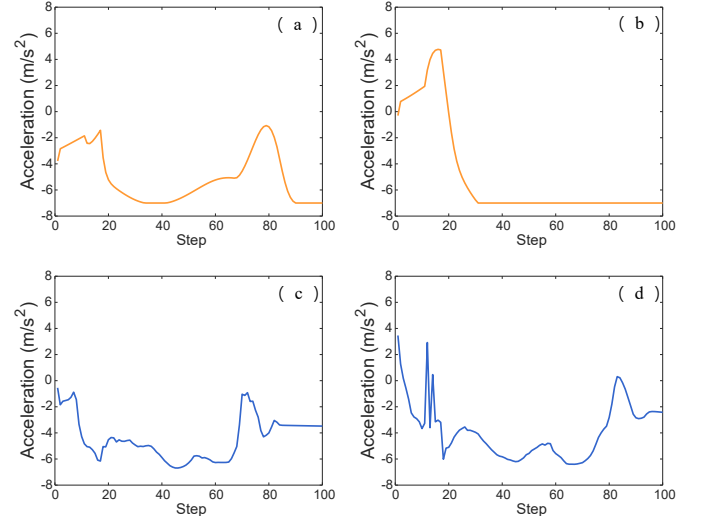


Fig. 7. Acceleration/deceleration profiles under two different scenarios. (a) PPO, Scenario 1. (b) PPO, Scenario 2. (c) SAC, Scenario 1. (d) SAC, Scenario 2.

for the standalone DRL model as function of total distance. Here, to capture potential suboptimal DRL strategies that may occur in practice, we considered a PPO model obtained from training where convergence has not occurred. According to Algorithm 1, the hybrid approach consistently selects the strategy that results in lower harm, which is depicted in blue.

To further validate the effectiveness of the proposed hybrid method, we conduct comparative experiments with standalone DRL and E-V2X-BM strategies, using identical simulation settings. Performance is measured under varying IVD conditions ($d_1(0), d_2(0)$ in the range [5, 10] m) over 5,000 test episodes with a fixed random seed. To highlight the importance of incorporating a safety bound, we considered a PPO model obtained from training before convergence occurred.

The results are summarized in Table II. The hybrid method achieves the lowest number of average harm, collisions, and

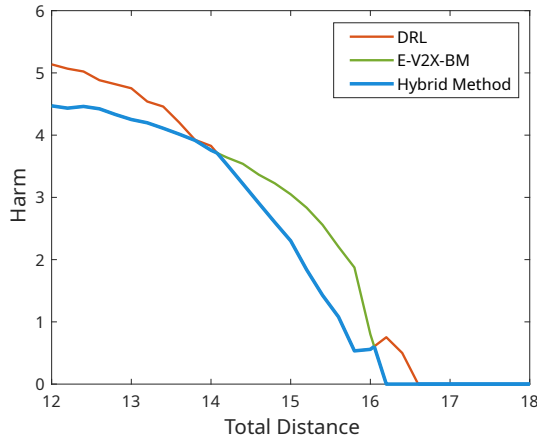


Fig. 8. Illustration of the hybrid method. Parameters for simulation are the same as for Fig.4.

TABLE II
PERFORMANCE OF E-V2X-BM, DRL, AND HYBRID STRATEGIES

| Metric | E-V2X-BM | Standalone DRL | Hybrid method |
|----------------------|----------|----------------|---------------|
| Number of collisions | 4263 | 3737 | 2995 |
| Collision rate | 85.26% | 74.74% | 59.9% |
| Average Harm | 9.8514 | 12.229 | 7.3641 |

TABLE III
COMPARISON OF FOUR DIFFERENT STRATEGIES (RANDOM TEST)

| Metric | Non-E | E-V2X-BM | SAC | PPO |
|----------------------|---------|----------|--------|--------|
| Number of collisions | 9391 | 8520 | 5896 | 5974 |
| Collision rate | 93.91% | 85.2% | 58.96% | 59.74% |
| Average Harm | 33.5878 | 9.8772 | 5.7001 | 5.6202 |
| Harm decrease | 0% | 70.59% | 83.02% | 83.26% |

collision rate (which is the fraction of scenarios ending in collisions). It is outperforming both the E-V2X-BM-only baseline and the standalone DRL model.

To further demonstrate the effectiveness of DRL in mitigating collision severity, we considered scenarios where $d_1(0)$ and $d_2(0)$ were randomly sampled in the interval $[5, 10]$ m, and $v_1(0), v_2(0), v_3(0)$ were randomly sampled in the interval $[18, 22]$ m/s. This setting was chosen to examine scenarios with small IVDs and moderate-speed vehicle-following, where the advantages of DRL are expected to be most pronounced. All other parameters are identical to those in Figure 4. A total of 10,000 random scenarios were generated. In each scenario, the performance of the non-ethical method (denoted as Non-E), E-V2X-BM, and the hybrid methods based on SAC and PPO was evaluated. For each method, the number of collisions, collision rate, and the average harm were computed, followed by calculation of the reduction in harm relative to the non-ethical method. The results are summarized in Table III.

The non-ethical method has the highest number of collision episodes (9391) and collision rate (93.91%), along with the largest average harm (33.5878). The E-V2X-BM method reduces both collision number and average harm, achieving a harm decrease ratio of 70.59% relatively to non-ethical method. Hybrid methods based on SAC and PPO demonstrate the best overall performance, with collision rates of 58.96% and 59.74%, respectively, and the lowest average harm values (5.7001 for SAC and 5.6202 for PPO). Both hybrid methods, based on SAC and PPO, achieve over 83% reduction in harm compared with the non-ethical method, indicating DRL superior capability in mitigating collisions and minimizing severity.

V. CONCLUSIONS

The paper demonstrates that Deep Reinforcement Learning (DRL) can significantly enhance safety in multi-vehicle-following scenarios. Two algorithms, Proximal Policy Optimization (PPO) and Soft Actor-Critic (SAC), were evaluated for deriving effective emergency braking strategies. Furthermore, a hybrid approach was proposed to improve the reliability and robustness of the DRL-based policies by integrating them with a conservative safety bound. Results show that combining DRL with the safety bound significantly reduces the collision rate and average collision severity/harm in situations with potential collision risks. Overall, the proposed hybrid method achieves superior safety and demonstrates potential for practical deployment.

REFERENCES

- [1] P. Ghorai, A. Eskandarian, M. Abbas, and A. Nayak, "A causation analysis of autonomous vehicle crashes," *IEEE Intelligent Transportation Systems Magazine*, vol. 16, no. 5, pp. 33–45, 2024.
- [2] A. Touran, M. A. Brackstone, and M. McDonald, "A collision model for safety evaluation of autonomous intelligent cruise control," *Accident Analysis & Prevention*, vol. 31, no. 5, pp. 567–578, 1999.
- [3] I. Taourati, A. Ramaswamy, J. Ibanez-Guzman, B. Monsuez, and A. Tappus, "Cross-cultural analysis of car-following dynamics: A comparative study of open-source trajectory datasets," in *2025 IEEE Intelligent Vehicles Symposium (IV)*, 2025, pp. 330–337.
- [4] G. Sidorenko, J. Thunberg, and A. Vinel, "Ethical v2x: Cooperative driving as the only ethical path to multi-vehicle safety," in *2023 IEEE 98th Vehicular Technology Conference (VTC2023-Fall)*. IEEE, 2023, pp. 1–6.
- [5] M. Geisslinger, F. Poszler, and M. Lienkamp, "An ethical trajectory planning algorithm for autonomous vehicles," *Nature Machine Intelligence*, vol. 5, no. 2, pp. 137–144, 2023.
- [6] C. Katrakazas, M. Quddus, W.-H. Chen, and L. Deka, "Real-time motion planning methods for autonomous on-road driving: State-of-the-art and future research directions," *Transportation Research Part C: Emerging Technologies*, vol. 60, pp. 416–442, 2015.
- [7] G. Sidorenko, J. Thunberg, and A. Vinel, "Cooperation for ethical autonomous driving," in *2024 20th International Conference on Wireless and Mobile Computing, Networking and Communications (WiMob)*. IEEE, 2024, pp. 391–395.
- [8] T. P. Lillicrap, J. J. Hunt, A. Pritzel, N. Heess, T. Erez, Y. Tassa, D. Silver, and D. Wierstra, "Continuous control with deep reinforcement learning," *arXiv preprint arXiv:1509.02971*, 2015.
- [9] V. Mnih, K. Kavukcuoglu, D. Silver, A. A. Rusu, J. Veness, M. G. Bellemare, A. Graves, M. A. Riedmiller, A. K. Fidjeland, G. Ostrovski, S. Petersen, C. Beattie, A. Sadik, I. Antonoglou, H. King, D. Kumaran, D. Wierstra, S. Legg, and D. Hassabis, "Human-level control through deep reinforcement learning," *Nature*, vol. 518, pp. 529–533, 2015.
- [10] S. Aradi, "Survey of deep reinforcement learning for motion planning of autonomous vehicles," *IEEE Transactions on Intelligent Transportation Systems*, vol. 23, no. 2, pp. 740–759, 2022.

[11] T. P. Lillicrap, J. J. Hunt, A. Pritzel, N. Heess, T. Erez, Y. Tassa, D. Silver, and D. Wierstra, “Continuous control with deep reinforcement learning,” *arXiv preprint arXiv:1509.02971*, 2015.

[12] J. L. Vermeulen, A. Hillebrand, and R. Geraerts, “Annotating traversable gaps in walkable environments,” in *2018 IEEE International Conference on Robotics and Automation (ICRA)*, 2018, pp. 3045–3052.

[13] A. Kendall, J. Hawke, D. Janz, P. Mazur, D. Reda, J.-M. Allen, V.-D. Lam, A. Bewley, and A. Shah, “Learning to drive in a day,” in *2019 international conference on robotics and automation (ICRA)*. IEEE, 2019, pp. 8248–8254.

[14] R. Eshleman and R. Singh, “Reconstructing the temporal progression of biological data using cluster spanning trees,” *IEEE Transactions on NanoBioscience*, vol. 16, no. 2, pp. 140–147, 2017.

[15] I. Taourati, A. Ramaswamy, J. Ibanez-Guzman, B. Monsuez, and A. Tapus, “Cross-cultural analysis of car-following dynamics: A comparative study of open-source trajectory datasets,” in *2025 IEEE Intelligent Vehicles Symposium (IV)*, 2025, pp. 330–337.

[16] P. F. Orzechowski, K. Li, and M. Lauer, “Towards responsibility-sensitive safety of automated vehicles with reachable set analysis,” in *2019 IEEE International Conference on Connected Vehicles and Expo (ICCVE)*, 2019, pp. 1–6.

[17] L. Li, G. Lu, Y. Wang, and D. Tian, “A rear-end collision avoidance system of connected vehicles,” in *17th International IEEE Conference on Intelligent Transportation Systems (ITSC)*, 2014, pp. 63–68.

[18] S. Chen, J. Hu, Y. Shi, Y. Peng, J. Fang, R. Zhao, and L. Zhao, “Vehicle-to-everything (v2x) services supported by lte-based systems and 5g,” *IEEE Communications Standards Magazine*, vol. 1, no. 2, pp. 70–76, 2017.

[19] Y. Wang, G. Tan, and H. Si, “Decision modeling for automated driving in dilemmas based on bidirectional value alignment of moral theory values and fair human moral values,” *Transportation Research Part F: Traffic Psychology and Behaviour*, vol. 108, pp. 14–27, 2025.

[20] D. J. Gabauer and H. C. Gabler, “Comparison of roadside crash injury metrics using event data recorders,” *Accident Analysis & Prevention*, vol. 40, no. 2, pp. 548–558, 2008.

[21] J. Zhang, C. Liang, S. Yu, R. Liu, and J. Gao, “Consistency of calculation results of two typical vehicle collision models,” *Procedia Engineering*, vol. 137, pp. 220–224, 2016, green Intelligent Transportation System and Safety.

[22] T. Semple and G. Fountas, “Twelve years of evidence: modelling the injury severity of single-vehicle collisions pre- and post-20mph (32 km/h) implementation in edinburgh and glasgow,” *Accident Analysis & Prevention*, vol. 221, p. 108183, 2025.

[23] A. F. Tencer, “Low speed rear end automobile collisions and whiplash injury, the biomechanical approach,” *Medicine, Law & Society*, vol. 12, no. 2, p. 1–20, Oct. 2019.

[24] L. Crosato, H. P. H. Shum, E. S. L. Ho, and C. Wei, “Interaction-aware decision-making for automated vehicles using social value orientation,” *IEEE Transactions on Intelligent Vehicles*, vol. 8, no. 2, pp. 1339–1349, 2023.

[25] C. Yu, X. Wang, X. Xu, M. Zhang, H. Ge, J. Ren, L. Sun, B. Chen, and G. Tan, “Distributed multiagent coordinated learning for autonomous driving in highways based on dynamic coordination graphs,” *IEEE Transactions on Intelligent Transportation Systems*, vol. 21, no. 2, pp. 735–748, 2020.

[26] A. Kendall, J. Hawke, D. Janz, P. Mazur, D. Reda, J.-M. Allen, V.-D. Lam, A. Bewley, and A. Shah, “Learning to drive in a day,” in *2019 international conference on robotics and automation (ICRA)*. IEEE, 2019, pp. 8248–8254.

[27] B. R. Kiran, I. Sobh, V. Talpaert, P. Mannion, A. A. Al Sallab, S. Yoganmani, and P. Pérez, “Deep reinforcement learning for autonomous driving: A survey,” *IEEE transactions on intelligent transportation systems*, vol. 23, no. 6, pp. 4909–4926, 2021.

[28] A. Hazra, V. M. R. Tummala, N. Mazumdar, D. K. Sah, and M. Adhikari, “Deep reinforcement learning in edge networks: Challenges and future directions,” *Physical Communication*, vol. 66, p. 102460, 2024.

[29] E. Puiutta and E. M. Veith, “Explainable reinforcement learning: A survey,” in *International cross-domain conference for machine learning and knowledge extraction*. Springer, 2020, pp. 77–95.

[30] J. Schulman, F. Wolski, P. Dhariwal, A. Radford, and O. Klimov, “Proximal policy optimization algorithms,” *arXiv preprint arXiv:1707.06347*, 2017.

[31] T. Haarnoja, A. Zhou, P. Abbeel, and S. Levine, “Soft actor-critic: Off-policy maximum entropy deep reinforcement learning with a stochastic actor,” in *International conference on machine learning*. Pmlr, 2018, pp. 1861–1870.

[32] T. Haarnoja, A. Zhou, K. Hartikainen, G. Tucker, S. Ha, J. Tan, V. Kumar, H. Zhu, A. Gupta, P. Abbeel *et al.*, “Soft actor-critic algorithms and applications,” *arXiv preprint arXiv:1812.05905*, 2018.

[33] D. Silver, R. Sutton, and M. Müller, “Reinforcement learning of local shape in the game of go,” in *Proceedings of the 20th International Joint Conference on Artificial Intelligence*, ser. IJCAI’07. San Francisco, CA, USA: Morgan Kaufmann Publishers Inc., 2007, p. 1053–1058.

[34] A. Y. Ng, D. Harada, and S. J. Russell, “Policy invariance under reward transformations: Theory and application to reward shaping,” in *Proceedings of the Sixteenth International Conference on Machine Learning*, ser. ICML ’99. San Francisco, CA, USA: Morgan Kaufmann Publishers Inc., 1999, p. 278–287.

[35] S. Zhang and R. S. Sutton, “A deeper look at experience replay,” *arXiv preprint arXiv:1712.01275*, 2017.